Acta Materialia Transylvanica 8/2. (2025) 74–80.
DOI: Hungarian: https://doi.org/10.33923/amt-2025-02-06
English: https://doi.org/10.33924/amt-2025-02-06

ACTA MATERIALIA TRANSYLVANICA

Consequences of the Asymmetric Cutting of S355 Steel Grade when Using Acetylene and Hydrogen Combustible Gases

János KUTI,[1] Péter PATÓ,[2] Enikő Réka FÁBIÁN,[3] Andrea SZABÓ[4]

[1] *Óbuda University, Doctoral School on Materials Sciences and Technologies, Budapest, Hungary, kuti.janos@bgk.uni-obuda.hu*

[2] *Óbuda University, Bánki Donát Faculty of Mechanical and Safety Engineering, Institute for Natural Sciences and Basic Subjects. Budapest, Hungary, pato.peter@bgk.uni-obuda.hu*

[3] *Óbuda University, Bánki Donát Faculty of Mechanical and Safety Engineering, Institute of Materials and Manufacturing Sciences, Department of Material Technology. Budapest, Hungary, fabian.reka@bgk.uni-obuda.hu*

[4] *University of Dunaújváros., Technical Institute, Dunaújváros, Magyarország, szaboandrea@uniduna.hu*

Abstract

In this research, flame cutting experiments were performed on 35 mm thick S355JR steel plates using acetylene and hydrogen. During our tests, we cut the pieces so that we ended up with one much larger piece and one smaller piece. Changes in the microstructure and hardness were studied, according to the size of the pieces and the cutting position, using the two different fuel gases. The heat flow of the smaller piece was measured using thermocouples.

Keywords: *flame cutting, non-alloy structural steels..*

1. Introduction

The S355JR is a non-alloy, structural steel grade defined in the EN 10025-2:2020 standard. The S355 grade belongs to the group of structural steels; as indicated by its designation ("S"), while the number denotes the minimum yield strength. Accordingly, its minimum yield strength is 355 MPa up to a plate thickness of 16 mm. As the thickness increases, the yield strength decreases progressively; in the case of the 35 mm thick plate used for the experiments in this study, the minimum yield strength is 335 MPa.

The suffix "JR" specifies the steel's toughness determined by the Charpy impact test at a defined temperature at which the material exhibits a minimum impact energy of 27 J. In this case, the specified test temperature is +20 °C. From a chemical composition perspective, S355 JR is a non-alloy, low-carbon steel. Its carbon equivalent is approximately 0.45 **[1, 2]**.

During flame cutting, the fuel gas mixed with oxygen is burned in a high-pressure oxygen jet, heating the material to its ignition temperature (preheating), while simultaneously blowing away the resulting molten combustion products with the oxygen jet. The conditions for the applicability of flame cutting are that: the material must be combustible in oxygen; the ignition temperature of the material must be lower than its melting point; the melting point of the oxide formed from the material is also lower than its melting point, so that the combustion products can be brought to a molten state and easily removed from the cutting gap; the combustion heat (heat of oxidation) of the material should be high and its thermal conductivity low so that the cutting gap forms quickly and remains narrow.. In industrial practice, these flame cutting requirements are only applied to unalloyed and low-alloy structural steels and cast steel. Although the ignition point of unalloyed steels remains below the melting point of the material up to a carbon content of nearly 2%, they can typically be cut very efficiently with a flame up to a carbon content of 0.25% **[3, 4]**.

Low-carbon (C < 0.25%), unalloyed, and mildly alloyed structural steels are used in large quantities for the manufacture of welded structures, and this trend is expected to grow significantly in the coming years [5]. The most commonly used combustible gas for flame cutting is acetylene (C_2H_2), but hydrogen is also playing an increasingly important role due to environmental considerations [6, 7, 8].

2. Flame Cutting of Test Specimens

The flame cutting of the test specimens used in our research was carried out in the demonstration laboratory of Messer Hungarogas Ltd. For the investigations, we used S355JR steel with a 35 mm plate thickness, cut into 200 × 300 mm specimens. Two test plates were cut: one using acetylene as the fuel gas, and the other using hydrogen. During cutting, maintaining a uniform cutting speed was essential from several perspectives; this was ensured by a flame-cutting torch mounted on a mechanical cutting carriage (Fig. 1).

The dimensions of the plates used as test specimens are shown in Fig. 2. The hardness test specimens are numbered from 1 to 4; these numbers are used throughout the remainder of the paper to identify the individual samples. The cutting kerfs were initiated between samples 1 and 2 - smallest and largest part of cut pieces (sections with widths of 20 mm and 180 mm). The specimens taken from the plate cut with acetylene as the fuel gas are designated with the letter “A” preceding the number (test specimens A1, A2, A3, and A4), whereas those taken from the plate cut using hydrogen are identified with the prefix “H” (samples H1, H2, H3, and H4). (Fig. 3). All test specimens were extracted from the plates using waterjet cutting to avoid additional microstructural alterations. Hardness measurements were performed perpendicular to the flame-cut surface, as a function of the distance from the cut edge, following appropriate surface preparation.

Another important aspect during cutting is maintaining the appropriate gas flow rates, which were verified prior to the process using a flow meter Table 1 summarizes the key parameter values recorded during the cutting operation.

Table 1. *Set parameters at the flame-cutting process*

Parameter	Acetylene cutting	Hydrogen cutting
Cutting speed (mm/min)	520	520
Fuel gas flow rate (L/min)	1.6	1.2
Cutting oxygen flow rate (L/min)	5.1	5.1

Fig. 1. *Flame-cutting equipment used for preparing the test specimens.*

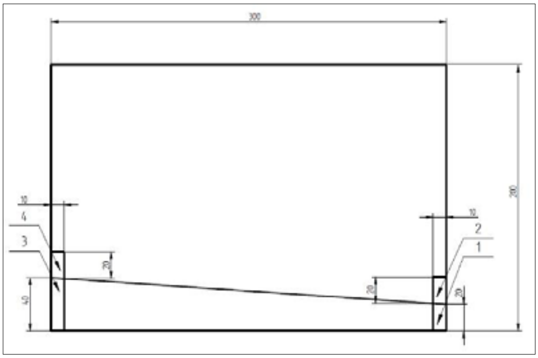

Fig. 2. *Layout of the test plate showing the cut edge and the positions of the test specimens.*

Fig. 3. *Photograph of the test specimen after cutting.*

3. Thermocouple measurements

Before cutting, thermocouples were inserted into the plates to enable continuous monitoring of the temperature during the process. The thermocouples were positioned along the side of the plate, near the cutting line, as illustrated in Fig. 4. As can be seen on Figure 4, the thermocouples are numbered from 1 to 8. The thermocouples

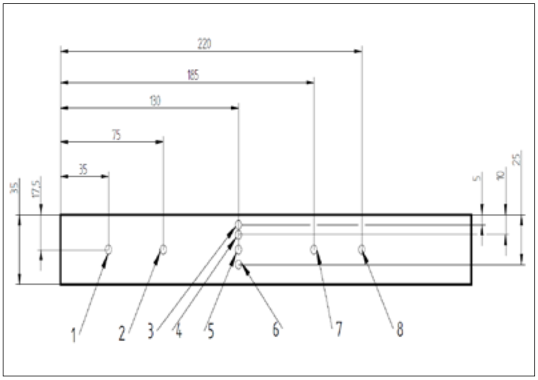

Fig. 4. *Position of the thermocouples along the side of the plate.*

numbered 1, 2, 5, 7, 8 were positioned in middle of plate thickness at 35 mm, 75 mm, 130 mm, 185 mm and 220 mm from the end of cut kerf. The thermocouples 3, 4, 5 and 6 were positioned at 170 mm from the beginning of cut kerf, at a different distance from the face of plate (5 mm, 10 mm, 17,5 mm and 25 mm). For easier identification when presenting the measurement results, the thermocouple numbers are prefixed with the letters "A" or "H", corresponding to acetylene and hydrogen fuel gas usage, respectively (i.e., A1–A8 and H1–H8).

For the measurements, TC Direkt brand, Type K, stainless-steel sheathed thermocouples were used, with a diameter of 1 mm and a length of 300 mm. The thermocouples were placed in drilled holes at a depth of 18 mm inside the plate material, positioned so that their tips were in contact with the end of each borehole. The holes were drilled to a diameter of 3.5 mm down to 16 mm, followed by an additional 2 mm of drilling with a 1.1 mm diameter. This ensured stable positioning of the thermocouples within the bores.

For recording the data supplied by the thermocouples, a DATAQ DI-710-EH multi-channel Ethernet-based data acquisition unit for analog signals was used. The device operated with the manufacturer's free software, WinDaq, which enabled exporting the results in tabular format.

4. Hardness measurement. Microscopy

In order to determine how fuel gas affects the microstructure of the cutting environment and how the size of the cut pieces affects the microstructure, the hardness on polished samples was measured and the microstructure after etching with nitric acid was examined.

The hardness measurements were carried out in the materials testing laboratory of the University of Dunaújváros. A Buehler Wilson UH4750 hardness tester was used to determine the hardness values. Establishing the accuracy and reliability of the hardness tester used for the measurements is essential to ensure that no false measurement results are obtained. For this purpose, a trial measurement was performed on a reference block with a certified hardness value of 388.6 HV10, allowing the accuracy of the measuring device to be verified. After completing the instrument setup, the trial measurement was performed.

The microstructure was examined using a Zeiss Axio Observer Z1M optical microscope.

5. Results

5.1. Results of the thermocouple measurements

The temperature of the plate and its changes (cooling) during cutting were evaluated based on the data recorded by the thermocouples. The results are illustrated in Fig. 5 and 6. shown separately for the measurements obtained during cutting with acetylene and hydrogen. Fig. 5 shows the values recorded during cutting with acetylene, while Fig. 6 shows the values measured when hydrogen was used as fuel gas.

The measurement results show that from the start of cutting to 80 mm, the maximum temperature did not reach 200°C for either cutting gas. The maximum temperatures recorded by the thermocouples barely exceeded 300°C for both cutting gases. The two types of cutting gas did not cause any difference at the measurement points.

Based on these results, it is evident that the two plates reached nearly identical temperatures at the measurement points when using the two different fuel gases, and their temperature changes over time were also similar. The reasons for the differences observed in the resulting microstructural changes are discussed in the following subsections.

5.2. Results of the Hardness Measurements

The hardness measurements were performed using the Vickers method with a test load of 98.81 N. Each test specimen was measured at 10 positions, depending on the distance from the cut edge. The hardness measurements were taken at distances of 1, 2, 3, 4, 5, 7, 9, and 15 mm from the cut edge (Table 2. and 3.).

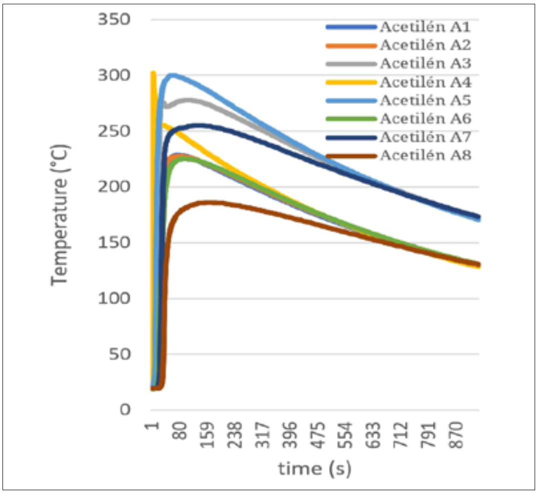

Fig. 5. *Cooling curves for acetylene cutting.*

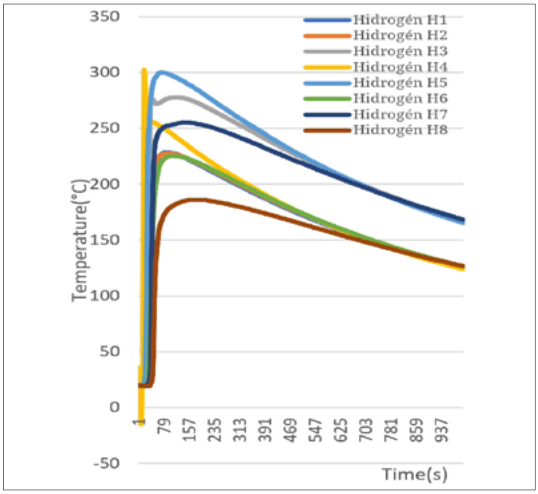

Fig. 6. *Cooling curves for hydrogen cutting*

Table 2. *Hardness values measured on the test specimens cut using acetylene as the fuel gas, as a function of distance from the cut edge*

Distance from flame cut edge (mm)	Hardness (HV10)			
	A1	A2	A3	A4
1	327.3	258.1	170.2	463.5
2	153.1	243.4	151.3	292.0
3	163.2	198.0	144.7	188.0
4	166.2	186.8	145.5	166.2
5	165.2	181.1	145.5	173.4
7	162.3	161.3	142.3	170.2
9	162.3	160.4	123.8	167.2
15	153.1	156.7	138.4	166.2

Table 3. *A hidrogén éghető gáz felhasználásával vágott próbatesteken mért keménységértékek a távolság függvényében*

Distance from flame cut edge (mm)	Hardness (HV10)			
	H1	H2	H3	H4
1	192.9	158.5	163.2	314.0
2	172.3	148.8	151.3	179.8
3	143.1	134.7	151.3	173.4
4	146.3	133.3	143.1	177.7
5	143.9	136.2	139.9	158.5
7	163.2	133.3	139.9	154.9
9	163.2	137.7	143.1	158.5
15	149.6	136.9	143.1	158.5

To compare the fuel gases used for cutting, it is necessary to evaluate the hardness values of selected test specimens against each other. This allows the differences in microstructural changes resulting from the use of different gases to be determined. The following figures present these comparisons separately. The hardness values measured on test specimens of identical positions—but cut using different fuel gases—were compared as a function of the distance from the cut edge.

From Fig. 7–10, it can be observed that at the beginning of the cut, contrary to our expectations, the specimens with smaller mass and volume (samples numbered 1) exhibited higher hardness values. Initially, we assumed that the specimens with larger mass and volume would extract more heat, and therefore specimens 2 and 4 would develop higher hardness.

Specimen 4 shows higher hardness values near the cut edge—both for acetylene and hydrogen cutting—compared to specimen 3. This is due to the larger material mass located behind specimen 4, which extracts more heat from the cutting process. As a result, greater heat removal occurred there, leading to lower heating of those specimens.

For specimen 1, assuming that heat was transferred symmetrically into the two adjacent pieces, the smaller specimen received the same amount of heat input despite its lower mass. Consequently, it remained at elevated temperatures for a longer period. This allowed more extensive austenite formation and resulted in larger grain

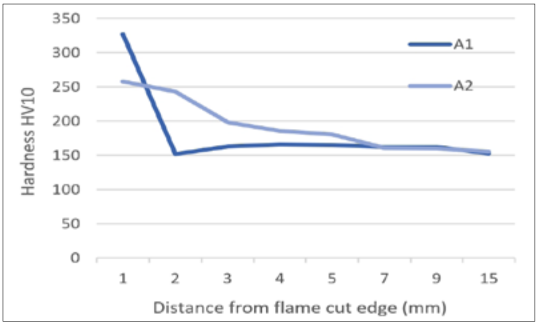

Fig. 7. *Comparison of hardness values measured on test specimens A1 and A2.*

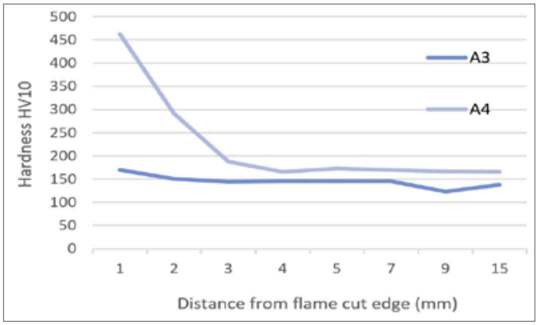

Fig. 8. *Comparison of hardness values measured on test specimens A3 and A4.*

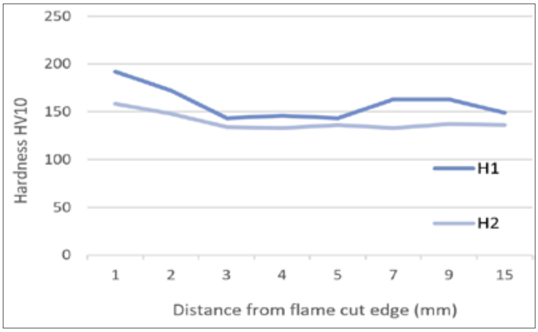

Fig. 9. *Comparison of hardness values measured on test specimens H1 and H2.*

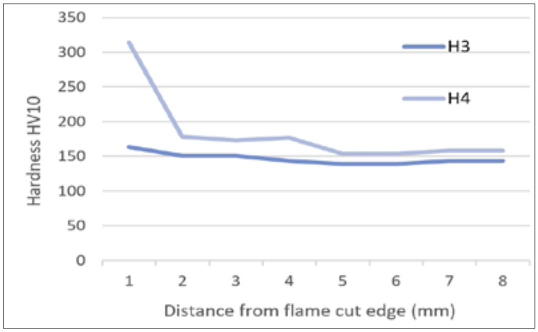

Fig. 10. *Comparison of hardness values measured on test specimens H3 and H4.*

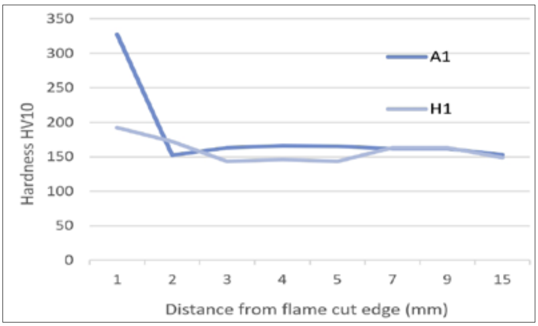

Fig. 11. *Comparison of hardness values measured on test specimens A1 and H1.*

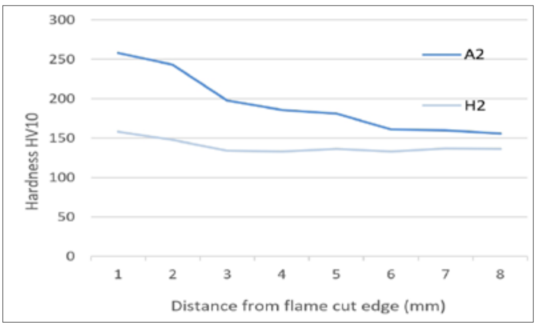

Fig. 12. *Comparison of hardness values measured on test specimens A2 and H2.*

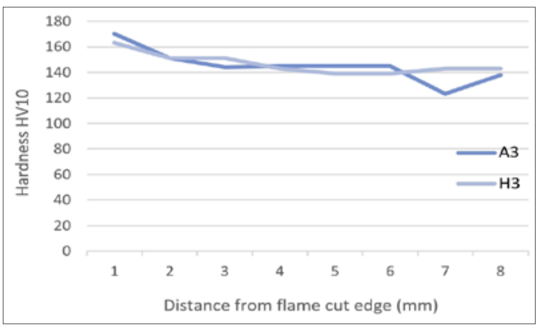

Fig. 13. *Comparison of hardness values measured on test specimens A3 and H3.*

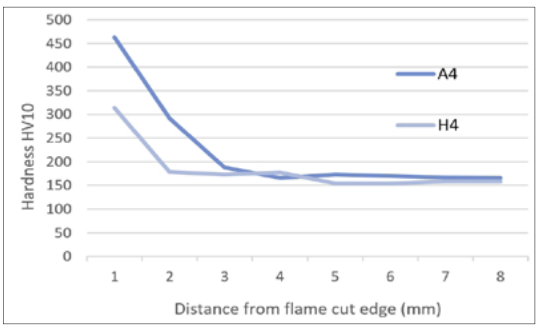

Fig. 14. *Comparison of hardness values measured on test specimens A4 and H4.*

sizes. Both effects promote the formation of martensite [9, 10].

From Fig. 11. and 12, it can be observed that at the beginning of the cut, the hardness values are significantly higher when acetylene is used compared to hydrogen. In Fig. 13 and 14, at the end of the cut, it can be seen that for the smaller specimen, both hydrogen and acetylene preheated the material prior to cutting. Due to the accumulated thermal energy, the resulting hardness values are nearly identical. For the larger specimen, however, the higher flame temperature of acetylene becomes more pronounced.

Based on hardness measurements, it can be concluded that in both acetylene and hydrogen cutting, the hardness of the 35 mm plate is practically the same as that of the base material when measured 6 mm from the cutting surface, but using hydrogen as fuel gas the heat affected zone is under 3 mm. This measurement is consistent with the results observed in high energy density cutting [11].

5.3. Metallographically studies results

Fig. 15 shows the basic microstructure of the plate material. The ferrite and pearlite bands formed as a result of rolling are clearly visible. Due to the rapid heating and cooling that occurs during cutting, the bands behave differently if they do not have time to homogenize.

Fig. 16. shows the microstructure of the A4 test specimen. The transitional microstructure of this test specimen can be seen on the base metal side, at the beginning of the heat-affected zone. It is noticeable that the base metal pearlite has been transformed. The originally pearlitic bands have been transformed into bainite and martensite.

Fig. 17. shows the microstructure of test specimen H1 near the cutting edge. Homogenization occurred only in the immediate vicinity of the cutting edge, but the microstructure in the heat-affected zone is neither ferritic nor pearlitic.

A higher resolution had to be used to determine the microstructure formed in the heat-affected zone.

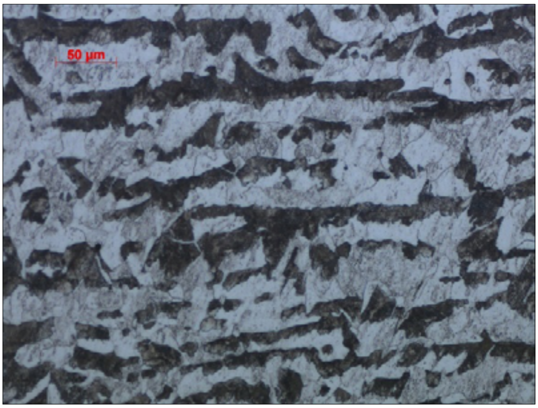

Fig. 15. *Base microstructure of the plate.*

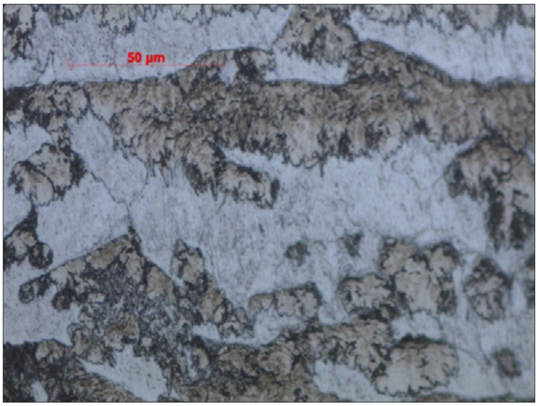

Fig. 16. *Heat-affected zone of specimen A4.*

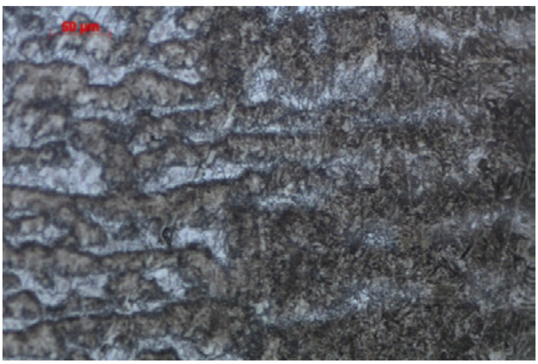

Fig. 17. *Transitional microstructure of specimen H1 adjacent to the cut zone.*

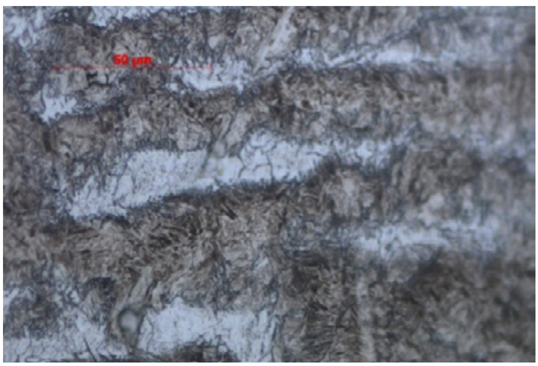

Fig. 18. *Heat-affected zone and microstructural boundary at the cut edge of specimen H1.*

Fig. 18. shows the heat-affected zone of sample H1. The original pearlite rows were transformed into martensite and bainite, and some carbide particles also appeared in the ferrite rows, but they remained essentially ferrite.

6. Conclusions

In this study, flame cutting with hydrogen and acetylene as fuel gases was compared using S355JR steel. At the beginning of the cut, contrary to our expectations, the specimens with smaller mass and volume (samples numbered 1) exhibited higher hardness values

However, according to the thermocouple measurements in the present experiments, this trend did not occur. Instead, the higher flame power and flame temperature of acetylene had a dominant influence on the resulting microstructural transformations.

References

[1] Meadinfo – Material properties of S355 steel. https://meadinfo.org/2015/08/s355-steel-properties.html

[2] Gáti J.: *Hegesztési zsebkönyv,*. Cokom Mérnökiroda Kft., Miskolc, 2003. 42–45.

[3] Bitay E.: *Hegesztési alapismeretek.* Erdélyi Múzeum-Egyesület, Kolozsvár, 2021. 87–89.

[4] Gáti J.: *Hegesztési Zsebkönyv I. Hegesztési eljárások.* Cokom Mérnökiroda Kft., Budapest, 2023. 151–158.

[5] Market Research Report, 2025. https://www.fortunebusinessinsights.com/industry-reports/welding-market-101657 (letöltve: 2025. december 16.)

[6] Hamzah A.: *Development of welding technology in the future: analysis of trends and impacts on industry and the environment.* Collaborate Eng. Daily Book Series 1. (2023) 100–106.

[7] Mehrifar Y., Zamanian Z., Pirami H.: *Respiratory exposure to toxic gases and metal fumes produced by welding processes and pulmonary function tests.* International Journal of Occupational Medicine and Environmental Health, 10/1. (2019) 40–49.
https://doi.org/10.15171/ijoem.2019.1540.

[8] Suban M., Tusek J., Uran M.: *Use of hydrogen in welding engineering in former times and today.* Journal of Materials Processing Technology, 119/1–3. (2001) 193–198.
https://doi.org/10.1016/s0924-0136(01)00956-6.

[9] Tisza Miklós: *Anyagvizsgálat*. Miskolci Egyetemi Kiadó, Miskolc, 2010.

[10] Callister William D., Rethwisch David G.: *Materials Science and Engineering.* John Wiley & Sons, Hoboken, New Jersey, USA, 2018.

[11] Diekhoff P., Sun J., Nitschke-Pagel T. et al.: *A comparative study of the thermal and mechanical cutting influence on the cut-edge hardness of structural steels S355 and S1100.* International Journal of Advanced Manufacturing Technology, 130. (2024) 5951–5964.
https://doi.org/10.1007/s00170-023-12937-2